ChemPubSoc Europe

DOI: 10.1002/slct.201702083

Chemistry SELECT Full Papers

Catalysis

Palladium Nanoparticle-Immobilized Porous Polyurethane Material for Quick and Efficient Heterogeneous Catalysis of Suzuki-Miyaura Cross-Coupling Reaction at Room Temperature

Sandeep Kumar Dey,[a, b] Dennis Dietrich,[a] Susann Wegner,[a] Beatriz Gil-Hernández,[a] Sarvesh Shyam Harmalkar,[b] Nader de Sousa Amadeu,[a] and Christoph Janiak*[a]

Here we report, room temperature heterogeneous catalysis of the Suzuki-Miyaura cross-coupling reaction by a Pd^0 nanoparticle-immobilized porous organic polymer (**TPU-Pd**), providing excellent yields (up to 99%) using low catalyst loading. High nitrogen- and oxygen-donor content of triazine-based porous polyurethane (**TPU**) makes it an efficient porous polymer for Pd-immobilization and subsequent heterogeneous catalysis of C–C cross-coupling reactions. X-ray photoelectron spectroscopy of **TPU-Pd** showed characteristic binding energy peaks of Pd^0. Atomic absorption spectroscopy revealed 10.4 wt% of Pd^0 in **TPU-Pd**, and transmission electron microscopy images showed well-dispersed and facetted Pd^0 nanoparticles of size 5–20 nm. Catalysis of Suzuki-Miyaura reaction was observed to be completed in 3 h at 25 °C for a wide range of aryl halide substrates with phenylboronic acid, whereas increasing the reaction temperature to 80 °C largely allows decreasing the reaction time to 0.5-1 h. The porosity and surface area of the catalyst was not affected after catalysis, and the catalyst has been reused for five consecutive runs.

Introduction

Over the last decade rapid development has been achieved on the rational design and synthesis of porous organic polymers (POPs) based on their applications in the field of gas storage and separation, water sorption, catalysis, and optoelectronics.[1] From catalysis point of view, nitrogen rich crystalline and amorphous POPs have been efficiently employed as heterogeneous organocatalysts for aldol-type C–C bond forming reactions and conjugate addition reactions.[2] Moreover, POPs having suitable chemical functionalities and permanent porosity can act as versatile and efficient supports for various catalytically active metals. Along this line, imine-based and triazine-based POPs have been established as suitable candidates for anchoring and immobilizing noble metal ions such as, palladium (Pd), platinum (Pt), ruthenium (Ru) and gold (Au) within the porous framework.[3] These hybrid metal-grafted POP materials have been used to carry out heterogeneous catalysis of several important organic reactions, often with excellent catalytic activity and recyclability.[3] In recent years, both microporous and mesoporous Pd-immobilized (Pd^{2+} ions or Pd^0 nanoparticles) POPs have been shown to catalyze some representative Pd-catalyzed reactions, such as the Suzuki-Miyaura (Scheme 1),[4] Heck/Sonogashira[4e,5] and Hiyama[6]

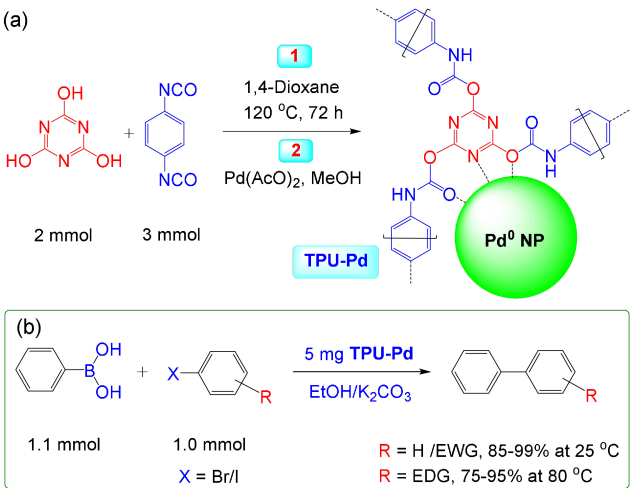

Scheme 1. (a) Solvothermal synthesis of triazine-based porous polyurethane (**TPU**), and its post-synthetic functionalization with palladium acetate to obtain Pd^0-immobilized **TPU** (**TPU-Pd**), (b) **TPU-Pd** catalysed *Suzuki-Miyaura cross-coupling* reaction of phenylboronic acid with various aryl halide substrates at 25 °C and 80 °C (EWG = electron withdrawing group, and EDG = electron donating group, see Table 1).

[a] *Dr. S. K. Dey, D. Dietrich, S. Wegner, Dr. B. Gil-Hernández, Dr. N. de Sousa Amadeu, Prof. Dr. C. Janiak*
Institut für Anorganische Chemie und Strukturchemie
Heinrich-Heine-Universität Düsseldorf
40225 Düsseldorf, Germany
Fax: +49-211-81-12287
Tel: +49-211-81-12286
E-mail: janiak@uni-duesseldorf.de
[b] *Dr. S. K. Dey, S. S. Harmalkar*
Department of Chemistry
Goa University
Taleigao Plateau, Goa 403206, India

Supporting information for this article is available on the WWW under https://doi.org/10.1002/slct.201702083

cross-coupling reactions. The difficulty in separating and recycling the expensive Pd^{2+} salt catalysts applied in homogeneous reaction media eventually demands for an efficient and recyclable heterogeneous catalyst for the Pd-catalyzed reactions, preferably under ambient and sustainable conditions.

The Pd-catalyzed Suzuki-Miyaura (S–M) cross-coupling reaction of aryl halides with arylboronic acid is one of the most efficient methods for the synthesis of biaryls, triaryls or introduction of substituted aryl moieties in organic synthesis. Although, several Pd-grafted POPs have been used for S–M reaction,[4] a quick and efficient heterogeneous catalysis of this reaction by a Pd-POP catalyst at room temperature under environmentally benign conditions has not been reported. All reported S–M cross-coupling reactions catalyzed by Pd-grafted POPs have employed a temperature of 60 °C or above (up to 150 °C) using ethanol-water solvent mixture in most cases (Table S4 in the Supporting Information).[4] Several post-modified Pd-grafted MOFs and other Pd-grafted porous materials like porous carbon and silica have also been used for heterogeneous S–M catalysis (Table S4, in the Supporting Information).[7] To further add to this list, a couple of heterogeneous Pd-catalysts (nonporous) and metallodendritic grafted Fe_2O_3 nanoparticles have shown good recyclability and efficiency of catalyst.[8]

However, quick and efficient heterogeneous catalysis of S–M cross-coupling reaction by a Pd-grafted POP at room temperature under ambient conditions is not known, to the best of our knowledge.

Because of their biocompatibility and biodegradability, several porous polyurethane (PU) materials have been used for soft tissue engineering applications and also in biosensor and magnetic resonance imaging (MRI) applications.[9] In our attempt to design a heterogeneous solid support for noble metal catalyst, we have synthesized a triazine-based porous polyurethane (**TPU**) material and functionalized the material with Pd^0 nanoparticles (NPs) to obtain **TPU-Pd**, for the purpose of catalysis of the S–M cross-coupling reaction under ambient conditions (Scheme 1).[10] High nitrogen- and oxygen-donor content of **TPU** makes it an efficient porous polymer for Pd-immobilization and subsequent heterogeneous catalysis. Herein, we report the quick and efficient heterogeneous catalysis of the S–M cross-coupling reactions of aryl halides with phenylboronic acid by **TPU-Pd** at room temperature (25 °C) in ethanol, showing excellent conversions (up to 99%) for most of the bromobenzene and iodobenzene derivatives. The reactions of all aryl halide substrates with phenylboronic acid have also been carried out at 80 °C to examine the effect of temperature on the reaction rates, and to improve the performance of the few substrates giving poor yield at 25 °C.

Results and Discussion

The triazine-based porous polyurethane (**TPU**) was synthesized by the condensation of cyanuric acid and 1,4-phenylenediisocyanate in 1,4-dioxane at 120 °C under solvothermal conditions (Scheme 1 and experimental section below). FT-IR spectrum of **TPU** showed presence of the carbonyl (C=O) and triazine stretching bands at 1637 and 1559 cm^{-1} respectively, (Figure S3 in the Supporting Information) indicating formation of the urethane-linked polymer. However, a low intensity isocyanate (N=C=O) stretching band was observed at 2270 cm^{-1}, indicating the presence of a small percentage of unreacted N=C=O groups in **TPU**. Solid-state ^{13}C CP/MAS NMR spectrum of **TPU** further confirmed the presence of carbonyl carbon of the urethane group at 159 ppm, whereas other peaks at 137 and 128 ppm were assigned to aryl rings (Figure S7 in the Supporting Information). The powder X-ray diffraction (PXRD) pattern of **TPU** displays several peaks over a broad background of the amorphous **TPU** (Figure 1a). The broad peaks at around 2-theta 21° and between 26–30° can be matched with the PXRD patterns of presumably nanocrystals of 1,4-phenylenediisocyanate and cyanuric acid (See Fig. S63 and S64 in Supporting Information) which may remain occluded in the pores of **TPU**. Scanning electron microscopy (SEM) images revealed that **TPU** forms as small proliferated flakes, which are aggregated into an overall sponge-like morphology (Figure 2a and S11 in the Supporting Information). CHN analysis showed 19.2 wt% of nitrogen in **TPU** which makes it an ideal material for metal-immobilization (Table S1 in the Supporting Information). Thermogravimetric analysis (TGA) showed that no solvent molecules were included within the pores of **TPU**, and the material was stable up to 280 °C (Figure S24 in the Supporting Information).

A nitrogen sorption measurement at 77 K showed permanent porosity in **TPU** with a BET surface area of 124 $m^2\ g^{-1}$ (Table S3 in the Supporting Information) and a total pore volume of 0.26 $cm^3\ g^{-1}$, calculated by using the DFT method. The non-local density functional theory (NLDFT) pore size distribution curve indicated a significant fraction of mesopores (20-200 Å) in **TPU**, and only a small fraction of micropores centred at a diameter of 17 Å (Figure S19b in the Supporting Information; note that macropores are not accounted for in N_2 sorption measurements). The nitrogen sorption isotherms of porous polymers with a broad pore size distribution are often difficult to analyze as they consist of micropores, mesopores and even macropores in some cases, and thereby, give complex adsorption-desorption curves which are generally difficult to assign to a particular type of isotherm. Low nitrogen uptake by **TPU** at low relative pressure ($P/P_0 = < 0.1$) is due to the lack of abundant micropores, and a sharp rise at high pressure regions (P/P_0 = 0.8-1.0) indicates the pore filling phenomena of mesopores (2-50 nm) by a multilayer adsorption process (Figure S19a, in the Supporting Information).[4d,12c] The nitrogen sorption isotherm of **TPU** can be considered as a composite of Type II and Type III (mostly observed with nonporous or macroporous adsorbents), with a H4 hysteresis loop.[11] Hysteresis appearing in the multilayer range of physisorption isotherms is usually associated with capillary condensation in mesopore structures. A H4 hysteresis is generally observed for adsorbent particles with internal voids of irregular size and having a broad particle size distribution.[11] Therefore, a H4 hysteresis loop is a possible indication towards the presence of both mesopores and also towards aggregation induced

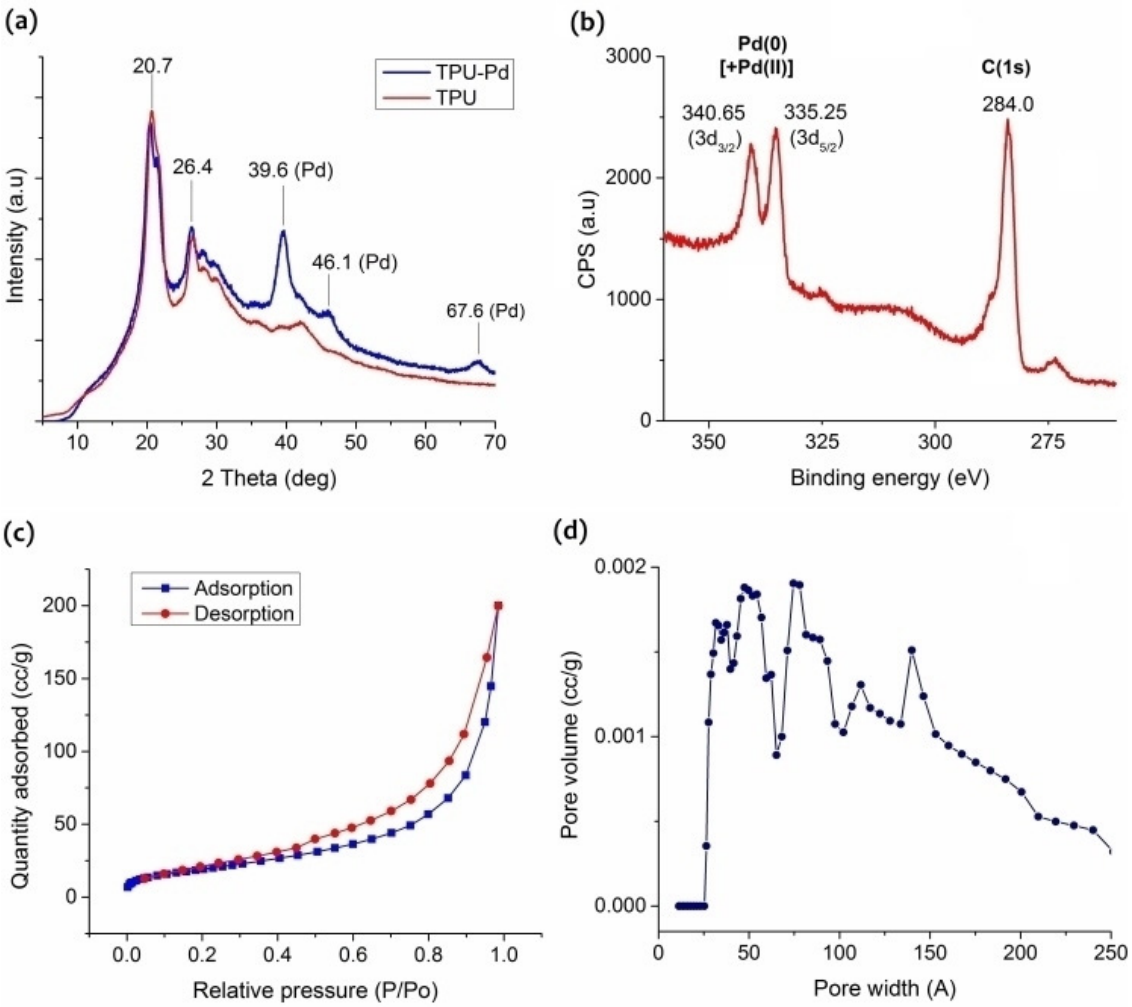

Figure 1. (a) PXRD patterns of **TPU** and **TPU-Pd**, (b) XP spectrum of **TPU-Pd** showing the presence of Pd(0); (c) Nitrogen sorption isotherm of **TPU-Pd** at 77 K, and (d) NLDFT pore size distribution curve of **TPU-Pd** using a slit pore model.

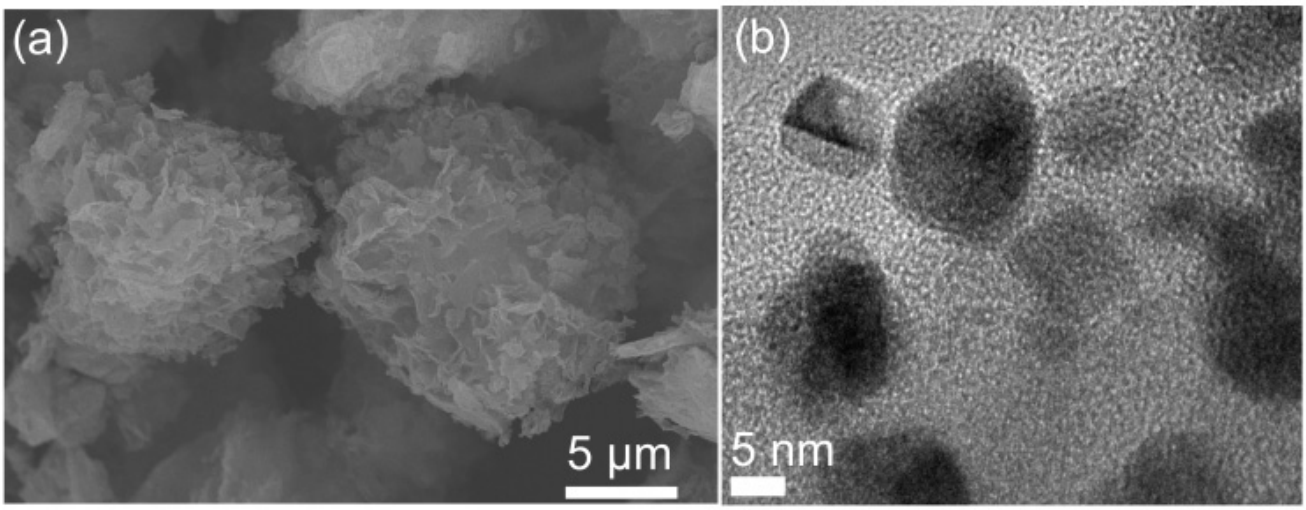

Figure 2. (a) SEM image of **TPU**, and (b) TEM image of **TPU-Pd**.

formation of slit like pores in the **TPU** material, as hinted in the SEM image (Figure 2a).

The unexpectedly low surface area of **TPU** results from the interpenetration in the polymeric network. The flexibility of the urethane groups and their tendency to form hydrogen bonds involving the carbonyl oxygen (C=O) and amide hydrogen (O=C-NH) is probably responsible for interpenetration during the framework formation. Framework interpenetration results in random orientation of the pores in the polymer giving a broad range of pore size distribution. Low BET surface area values have also been observed in related urea-based and amide-based porous organic polymers.[4f,12]

Simple post-treatment of **TPU** with palladium acetate, $Pd(AcO)_2$ in dichloromethane and then with methanol at room temperature afforded the Pd^0-immobilized **TPU** material, **TPU-Pd** (see Supporting Information).[5c,13] A comparison of the PXRD patterns and SEM images of **TPU** and **TPU-Pd** revealed that the structure of the material was well preserved after Pd^0-immobilization. The PXRD of **TPU-Pd** showed an additional intense peak at 39.6° and two broad peaks at 47.1° and 67.6° which can be assigned to (111), (200) and (220) crystal planes of Pd^0 nanoparticles (Figure 1a).[14] X-ray photoelectron spectroscopy (XPS) measurement of **TPU-Pd** confirmed that Pd^{2+} has been largely reduced to the Pd^0 metallic state.[13] The high-resolution XPS analysis shows a Pd(0) (335.5 and 341.1 eV for the $3d_{5/2}$ and $3d_{3/2}$ states) and a Pd(II) species (337.3 and 343.4 eV) with contributions of about 75% and 25%, respectively (Figure 1b and Figure S26 in the Supporting Information).[4c,5a] The well-dispersed and facetted Pd^0 NPs (size 5–20 nm) with distinct interference patterns (lattice planes) could be clearly observed in the TEM images of **TPU-Pd** (Figure 2b and Figure S29 in the Supporting Information). Selected area electron diffraction (SAED) showed sharp rings with reflections of the Pd^0 NPs, which are in good comparison with the cubic phase (Fm-3 m) of pure Pd^0 NPs (COD reference 1534921) (Figure S30 in the Supporting Information). Atomic absorption spectroscopy (AAS) of the dissolved Pd-species obtained after digesting **TPU-Pd** in aqua regia showed 10.4 wt% of Pd in **TPU-Pd**. A nitrogen sorption measurement (77 K) of **TPU-Pd** showed a decreased BET surface area of 80 $m^2\ g^{-1}$ (Figure 1c), however, without much affecting the total pore volume (0.25 $cm^3\ g^{-1}$) due to the predominantly mesoporous nature of the **TPU** material. A decrease in the BET surface area is consistent with the fact that Pd^0-immobilization partially occupies the pores in **TPU**. NLDFT pore size distribution curve of **TPU-Pd** showed the presence of only mesopores (20-200 Å), while the 17 Å micropores in **TPU** are not been observed anymore in **TPU-Pd** (Figure 1d). While a macro/mesoporous structure can accelerate the mass transfer of reactants and products, micropores of suitable size are favorable for anchoring metal particles.

To evaluate the catalytic activity of **TPU-Pd** for the S–M cross-coupling reaction, we have initially examined the reactions of phenylboronic acid (1.1 mmol) with 4-haloacetophenone (1.0 mmol) in ethanol at room temperature (aerobic condition) using K_2CO_3 as a base and 5 mg of **TPU-Pd** (0.5 mg, 4.7 μmol Pd). The reaction of 4-bromoacetophenone and 4-iodoacetophenone with phenylboronic acid was observed to be completed in 3 h giving 99% yield of 4-phenylacetophenone, as monitored by ^{1}H NMR spectroscopy (Figure S61 in the Supporting Information). Both bromobenzene and iodobenzene also afforded 99% of biphenyl under the same reaction conditions (Table 1). In the context of room temperature heterogeneous catalysis of S–M cross coupling reaction, Pd-NP immobilized metal organic frameworks (MOFs) namely MIL-101-Cr and MIL-101-Cr-NH_2 were shown to be efficient catalysts for the coupling of aryl halides with arylboronic acid at room temperature.[7a–b] Further, Pd-NP immobilized carbon nanotube was also found to be effective in promoting the coupling of aryl halides with arylboronic acid, providing good yields (75-98%) at room temperature.[7h] Table S4 in the supporting information provides a detailed comparison of reaction conditions of the S–M cross-coupling reactions catalyzed by different Pd-grafted heterogeneous porous catalysts and **TPU-Pd**. From Table S4, it is clear that the amount of **TPU-Pd** (0.5 mg, 4.7 μmol Pd for 1.0 mmol of aryl halide) used is significantly less when compared to the Pd-loading used for most of the Pd-grafted porous catalysts in S–M cross-coupling reaction.

Table 1. Catalytic data of **TPU-Pd** catalysed Suzuki-Miyaura cross-coupling reactions.

Aryl halides	Catalysis at 25 °C[a]		Catalysis at 80 °C[b]	
	Time/h	Yield, %[c]	Time/h	Yield, %[c]
1-bromobenzene	3	99[d]	0.5	99[d]
4-bromoacetophenone	3	99[d]	0.5	99[d]
3-bromoacetophenone	3	93[e]	0.5	95[e]
2-bromoacetophenone	3	99[d]	0.5	99[d]
4-bromobenzonitrile	3	99[d]	0.5	99[d]
1-bromo-4-nitrobenzene	3	99[d]	0.5	99[d]
1-bromo-4-fluorobenzene	3	99[d]	0.5	99[d]
methyl-4-bromobenzoate	3	99[d]	0.5	99[d]
2-bromoanisole	3	94[e]	1	95[e]
4-bromoanisole	3	30[e]	3	75[e]
2-bromotoluene	3	65[e]	2.5	93[e]
4-bromotoluene	3	30[e]	3	75[e]
1,3-dibromobenzene	3	50[e]	1.5	99[d]
1,4-dibromobenzene	3	n.d.[f]	1.5	99[d]
9-bromoanthracene	3	81[e]	1	99[d]
1-iodobenzene	3	99[d]	0.5	99[d]
4-iodoacetophenone	3	99[d]	0.5	99[d]
methyl-4-iodobenzoate	3	99[d]	0.5	99[d]
4-iodoacetanilide	3	85[e]	1	99[d]
4-iodoaniline	3	25[e]	3	88[e]

[a] General conditions: aryl halide (1.0 mmol), phenylboronic acid (135 mg, 1.1 mmol) in the presence of 5 mg **TPU-Pd** (0.5 mg, 4.7 μmol Pd) in ethanol at 25 °C, [b] general conditions: aryl halide (1.0 mmol), phenylboronic acid (135 mg, 1.1 mmol) in the presence of 5 mg **TPU-Pd** (0.5 mg, 4.7 μmol Pd) in ethanol at 80 °C, [c] yields reported are average of two independent runs under same conditions, [d] isolated yield, [e] yields corresponding to aryl halide conversion are based on ^{1}H NMR analysis of the isolated crude product (Figures S32-S62 in the Supporting Information), [f] yield could not be determined (n.d.) due to the complex nature of the ^{1}H-NMR spectrum.

Solvents have remarkable influences on the catalytic activity of **TPU-Pd**, as no biphenyl product was observed to be formed in aprotic solvents such as, acetonitrile and tetrahydrofuran under the same conditions. When the reaction was carried out

in neat water, only trace amounts of the desired product (~5%) were formed. According to the Pfizer solvent selection guide, ethanol is considered as a preferable choice of environmentally benign solvent if a reaction cannot be carried out in water medium.[15] Although there is a report where the S–M coupling has been carried out in neat water providing good yields of the desired product,[4f] but in our case, **TPU-Pd** catalyst worked most efficiently only in ethanol. To study the effect of temperature on the reaction kinetics, 4-bromoacetophenone and phenylboronic acid were allowed to react at 50 °C and 80 °C keeping all other reaction parameters the same. Quantitative yield (99%) of 4-phenylacetophenone was obtained within 1 h at 50 °C and in 0.5 h at 80 °C, indicative of faster reaction rate with gradual increase in temperature. The reaction of 4-bromoacetophenone with phenylboronic acid has also been carried out in gram scale (10 mmol) using **TPU-Pd** (50 mg), which yielded 99% product at room temperature within the same time frame of 3 h.

In order to validate the heterogeneity of the reaction, the filtrate from the reaction between 4-bromoacetophenone and phenylboronic acid (at 25 °C in ethanol for 3 h) has been analyzed by AAS to detect any Pd-leaching from **TPU-Pd**. No Pd was found within the detectable limit of AAS (0.22 mg/L). Furthermore, 4-bromoacetophenone and phenylboronic acid were allowed to react at room temperature for 1 h under standardized conditions (45% product yield), and the reaction mixture was filtered to remove the **TPU-Pd** catalyst. The filtrate was then stirred for another 2 h at room temperature, and ^{1}H NMR analysis of the isolated crude product showed no significant increase in the conversion to the desired product (49% product yield). These experiments suggested a strong interaction of Pd^0 NPs with **TPU** in **TPU-Pd**, and prove that the active phase was neither dissolved nor that active Pd^0 species leached from the **TPU** support. Further, to assess the heterogeneous pathway of **TPU-Pd** catalyst, poison experiments were carried out using carbon disulfide (CS_2), pyridine, and triphenyl phosphine (PPh_3) as poisoning additives. In the poison experiments which were carried out at room temperature, no catalytic activity of **TPU-Pd** was detected when the reaction of 4-bromoacetophenone and phenylboronic acid was performed in the presence of 45 μL (0.74 mmol) of carbon disulfide. CS_2 as a known catalyst poison binds strongly to active metal sites and blocks access to the substrates.[4f] Also addition of one equivalent of pyridine (relative to 4-bromoacetophenone) in the reaction mixture resulted in complete quenching of the cross-coupling reaction, whereas addition of one equivalent of triphenyl phosphine (relative to 4-bromoacetophenone) showed 89% quenching under the ideal reaction conditions (see Supporting Information). The incomplete quenching of the cross-coupling reaction is likely due to the fact that PPh_3 being a bulky molecule could not efficiently enter into the smaller pores of the frameworks to poison the palladium active sites.

To explore the substrate scope and generality of the catalytic system, a series of substituted aryl bromides and aryl iodides with different steric and electronic characters were tested under the given optimal conditions at 25 °C and 80 °C. In general, the reactivity of aryl halides with electron-withdrawing substituents (EWGs) was higher than that of electron-donating substituents (EDGs). The aryl halides with EWGs afforded the desired cross-coupling products in excellent yields (85-99%) at 25 °C (Table 1). Moderate to low yields (25-65%) were observed for the aryl halides with EDGs, except for 2-bromoanisole which yielded 94% of the desired product under the same conditions. However, the yield of the cross-coupling reactions between phenylboronic acid and aryl halides with EDGs can be significantly improved (75-95%) by increasing the reaction temperature to 80 °C (Table 1), which largely allows to decrease the reaction time to 0.5 or 1 h.

It is noted that the reactions of 2-bromoanisole and 2-bromotoluene with phenylboronic acid gave the desired products comparatively in much higher yield than 4-bromoanisole and 4-bromotoluene, suggesting that the electronic and steric nature of substituted aryl bromides have an effect on the cross-coupling reaction (Table 1). This was also reflected in the reactions of 2-, 3-, and 4-bromoacetophenone with phenylboronic acid where 2-bromoacetophenone and 4-bromoacetophenone gave 99% yield, and 3-bromoacetophenone yielded only 93% of the desired product (Table 1).

The catalyst was recycled and used for four consecutive runs with gradual loss in its activity for the cross-coupling reaction between 4-bromoacetophenone and phenylboronic acid at 25 °C (Figure S62 in the Supporting Information). No significant changes have been observed in the FT-IR, PXRD, TEM and XPS analysis data of the recycled **TPU-Pd** (see Supporting Information). Further, no significant decrease in the BET surface areas of recycled **TPU-Pd** samples have been observed from N_2 sorption measurements (Table S3 in the Supporting Information). However, SEM images showed that the flake like morphology of the aggregated crystals of **TPU-Pd** was slightly lost after the first catalysis run (Figure S12 in the Supporting Information), which perhaps affects the reaction yield in the consecutive runs. It is noted that, gradual decrease in the catalytic activity of Pd-grafted heterogeneous porous material is rather common and hence, the pursuit for a suitable Pd-grafted heterogeneous porous catalyst which would retain its catalytic activity for several cycles is utmost desirable.[4–7]

Conclusions

Overall in this contribution, we have shown the first instance of utilizing a Pd-nanoparticle immobilized porous polyurethane material for heterogeneous catalysis of the S–M cross-coupling reaction at room temperature, with high yield and some catalyst recyclability. The heterogeneous mesoporous structure of **TPU-Pd** catalyst allowed facile diffusion of organic reactant and product molecules in and out the pores during the reaction and thereby, facilitating faster reaction rate under mild conditions. Ambient condition, environmentally benign solvent, facile synthesis approach, gram scale synthesis, less reaction time, high yield and low catalyst loading (10 wt%, 0.5 mg, 4.7 μmol Pd in 5 mg composite) establish **TPU-Pd** as an excellent heterogeneous porous catalyst for the Suzuki-Miyaura cross-coupling reactions, when compared to the other known Pd-

grafted porous materials (Table S4 in the Supporting Information).[4,7]

Acknowledgements

Dr. Sandeep Kumar Dey gratefully acknowledges the Alexander von Humboldt foundation, Germany for awarding a postdoctoral research fellowship. We also acknowledge Dr. Raghavender Medishetty and Prof. Dr. Roland A. Fischer from Technical University of Munich for offering their help with thermogravimetric analysis of our samples. We thank Mrs. Laura Schmolke for measuring the high-resolution XPS.

Conflict of Interest

The authors declare no conflict of interest.

Keywords: cross-coupling reaction · heterogeneous catalysis · nanoparticle · palladium · porous material

[1] a) S.-Y. Ding, W. Wang, *Chem. Soc. Rev.* **2013**, *42*, 548–568; b) X. Feng, X. Ding, D. Jiang, *Chem. Soc. Rev.* **2012**, *41*, 6010–6022; c) Z. Xiang, D. Cao, L. Dai, *Polym. Chem.* **2015**, *6*, 1896–1911; d) J. L. Segura, M. J. Mancheno, F. Zamora, *Chem. Soc. Rev.* **2016**, *45*, 5635–5671.

[2] a) Q. Fang, S. Gu, J. Zheng, Z. Zhuang, S. Qiu, Y. Yan, *Angew. Chem. Int. Ed.* **2014**, *53*, 2878–2882; *Angew. Chem.* **2014**, *126*, 2922–2926; b) P. Kaur, J. T. Hupp, S. T. Nguyen, *ACS Catal.* **2011**, *1*, 819–835; c) D. B. Shinde, S. Kandambeth, P. Pachfule, R. R. Kumar, R. Banerjee, *Chem. Commun.* **2015**, *51*, 310–313; d) S. K. Dey, N. de Sousa Amadeu, C. Janiak, *Chem. Commun.* **2016**, *52*, 7834–7837; e) H. Xu, X. Chen, J. Gao, J. Lin, M. Addicoat, S. Irleb, D. Jiang, *Chem. Commun.* **2014**, *50*, 1292–1294.

[3] a) Y. Zhang, S. N. Riduan, *Chem. Soc. Rev.* **2012**, *41*, 2083–2094; b) P. Pachfule, S. Kandambeth, D. D. Diaz, R. Banerjee, *Chem. Commun.* **2014**, *50*, 3169–3172; c) S. Hug, M. E. Tauchert, S. Li, U. E. Pachmayr, B. V. Lotsch, *J. Mater. Chem.* **2012**, *22*, 13956–13964; d) R. Palkovits, M. Antonietti, P. Kuhn, A. Thomas, F. Schüth, *Angew. Chem. Int. Ed.* **2009**, *48*, 6909–6912; *Angew. Chem.* **2009**, *121*, 7042–7045; e) C. E. Chan-Thaw, A. Villa, L. Prati, A. Thomas, *Chem. Eur. J.* **2011**, *17*, 1052; f) J. Artz, R. Palkovits, *ChemSusChem.* **2015**, *8*, 3832–3838.

[4] a) M. K. Bhunia, S. K. Das, P. Pachfule, R. Banerjee, A. Bhaumik, *Dalton Trans.* **2012**, *41*, 1304–1311; b) C.-A. Wang, Y.-F. Han, Y.-W. Li, K. Nie, X.-L. Cheng, J.-P. Zhang, *RSC Adv.* **2016**, *6*, 34866–34871; c) S.-Y. Ding, J. Gao, Q. Wang, Y. Zhang, W.-G. Song, C.-Y. Su, W. Wang, *J. Am. Chem. Soc.* **2011**, *133*, 19816–19822; d) B. Li, Z. Guan, W. Wang, X. Yang, J. Hu, B. Tan, T. Li, *Adv. Mater.* **2012**, *24*, 3390–3395; e) A. Modak, J. Mondal, M. Sasidharan, A. Bhaumik, *Green Chem.* **2011**, *13*, 1317–1331; f) L. Li, Z. Chen, H. Zhong, R. Wang, *Chem. Eur. J.* **2014**, *20*, 3050–3060; g) C.-A. Wang, Y.-W. Li, X.-M. Hou, Y.-F. Han, K. Nie, J.-P. Zhang, *ChemistrySelect* **2016**, *1*, 1371–1376; h) V. Sadhasivam, R. Balasaravanan, C. Chithiraikumar, A. Siva, *ChemistrySelect* **2017**, *2*, 1063–1070.

[5] a) P. Pachfule, M. K. Panda, S. Kandambeth, S. M. Shivaprasad, D. D. Diaz, R. Banerjee, *J. Mater. Chem. A* **2014**, *2*, 7944–7952; b) A. Modak, M. Pramanik, S. Inagaki, A. Bhaumik, *J. Mater. Chem. A* **2014**, *2*, 11642–11650; c) D. Mullangi, S. Nandi, S. Shalini, S. Sreedhala, C. P. Vinod, R. Vaidhyanathan, *Sci. Rep.* **2015**, *5*, 10876; d) A. V. Nakhate, G. D. Yadav, *ChemistrySelect* **2016**, *1*, 3954–3965.

[6] a) S. Lin, Y. Hou, X. Deng, H. Wang, S. Suna, X. Zhang, *RSC Adv.* **2015**, *5*, 41017–41024; b) A. R. Hajipour, Z. Tavangar-Rizi, *ChemistrySelect* **2017**, *2*, 8990–8999.

[7] a) N. Shang, S. Gao, X. Zhou, C. Feng, Z. Wang, C. Wang, *RSC Adv.* **2014**, *4*, 54487–54493; b) V. Pascanu, Q. Yao, A. B. Gómez, M. Gustafsson, Y. Yun, W. Wan, L. Samain, X. Zou, B. Martín-Matute, *Chem. Eur. J.* **2013**, *19*, 17483–17493; c) Y. Huang, Z. Zheng, T. Liu, J. Lü, Z. Lin, H. Li, R. Cao, *Cat. Commun.* **2011**, *14*, 27–31; d) D. Saha, R. Sen, T. Maity, S. Koner, *Langmuir* **2013**, *29*, 3140–3151; e) R. Sen, D. Saha, S. Koner, P. Brandão, Z. Lin, *Chem. Eur. J.* **2015**, *21*, 5962–5971; f) F. Xamena, A. Abad, A. Corma, H. Garcia, *J. Catal.* **2007**, *250*, 294–298; g) W. Dong, L. Zhang, C. Wang, C. Feng, N. Shang, S. Gao, C. Wang, *RSC Adv.* **2016**, *6*, 37118–37123; h) D. V. Jawale, E. Gravel, C. Boudet, N. Shah, V. Geertsen, H. Li, I. N. N. Namboothiri, E. Doris, *Catal. Sci. Technol.* **2015**, *5*, 2388–2392; i) S. Jana, S. Haldar, S. Koner, *Tetrahedron Lett.* **2009**, *50*, 4820–4823; j) M. Cai, Q. Xu, Y. Huang, *J. Mol. Catal. A: Chem.* **2007**, *271*, 93–97; k) J. C. Park, E. Heo, A. Kim, M. Kim, K. H. Park, H. Song, *J. Phys. Chem. C* **2011**, *115*, 15772–15777.

[8] a) E. Hariprasad, T. P. Radhakrishnan, *ACS Catal.* **2012**, *2*, 1179–1186; b) Z. Wang, Y. Yu, Y. X. Zhang, S. Z. Li, H. Qian, Z. Y. Lin, *Green Chem.* **2015**, *17*, 413–420; c) D. Rosario-Amorin, M. Gaboyard, R. Clérac, L. Vellutini, S. Nlate, K. Heuzé, *Chem. Eur. J.* **2012**, *18*, 3305–3315.

[9] a) J. Guan, K. L. Fujimoto, M. S. Sacks, W. R. Wagner, *Biomaterials* **2005**, *26*, 3961–3971; b) Y.-C. Wang, F. Fang, Y.-K. Wu, X.-L. Ai, T. Lan, R.-C. Liang, Y. Zhang, N. M. Trishul, M. He, C. You, C. Yu, H. Tan, *RSC Adv.* **2016**, *6*, 3840–3849; c) A. Koh, Y. Lu, M. H. Schoenfisch, *Anal. Chem.* **2013**, *85*, 10488–10491; d) X. Zhang, Z. Du, W. Zou, H. Li, C. Zhang, S. Li, W. Guo, *RSC Adv.* **2015**, *5*, 65890–65896; d) S. Garmendia, D. Mantione, S. Alonso de Castro, C. Jehanno, L. Lezama, J. L. Hedrick, D. Mecerreyes, L. Salassa, H. Sardon, *Polym. Chem.* **2017**, *8*, 2693–2701.

[10] a) M. Akkoc, F. Imik, S. Yasar, V. Dorcet, T. Roisnel, C. Bruneau, I. Özdemir, *ChemistrySelect* **2017**, *2*, 5729–5734; b) X. Li, C. Liu, L. Wang, Q. Ye, Z. Jin, *ChemistrySelect* **2017**, *2*, 4016–4020.

[11] a) K. S. W. Sing, D. H. Everett, R. A. W. Haul, L. Moscou, R. A. Pierotti, J. Rouquerol, T. Siemeniewska, *Pure Appl. Chem.* **1985**, *57*, 603–619; b) M. Thommes, K. Kaneko, A. V. Neimark, J. P. Olivier, F. Rodriguez-Reinoso, J. Rouquerol, K. S. W. Sing, *Pure Appl. Chem.* **2015**, *87*, 1051–1062.

[12] a) V. M. Suresh, S. Bonakala, H. S. Atreya, S. Balasubramanian, T. K. Maji, *ACS Appl. Mater. Interfaces* **2014**, *6*, 4630–4637; b) S. Zulfiqar, M. I. Sarwar, C. T. Yavuz, *RSC Adv.* **2014**, *4*, 52263–52269; c) L. Rajput, R. Banerjee, *Cryst. Growth Des.* **2014**, *14*, 2729–2732; d) S. Zulfiqar, D. Mantione, O. E. Tall, M. I. Sarwar, F. Ruipérez, A. Rothenberger, D. Mecerreyes, *J. Mater. Chem. A* **2016**, *4*, 8190–8197

[13] T. A. Stephenson, S. M. Morehouse, A. R. Powell, J. P. Heffer, G. Wilkinson, *J. Chem. Soc.* **1965**, 3632–3640.

[14] W. Dong, L. Zhang, C. Wang, C. Feng, N. Shang, S. Gao, C. Wang, *RSC Adv.* **2016**, *6*, 37118–37123.

[15] K. Alfonsi, J. Colberg, P. J. Dunn, T. Fevig, S. Jennings, T. A. Johnson, H. P. Kleine, C. Knight, M. A. Nagy, D. A. Perry, M. Stefaniak, *Green Chem.* **2008**, *10*, 31–36.

Submitted: September 7, 2017
Revised: January 12, 2018
Accepted: January 15, 2017